



저작자표시-비영리-변경금지 2.0 대한민국

이용자는 아래의 조건을 따르는 경우에 한하여 자유롭게

- 이 저작물을 복제, 배포, 전송, 전시, 공연 및 방송할 수 있습니다.

다음과 같은 조건을 따라야 합니다:



저작자표시. 귀하는 원저작자를 표시하여야 합니다.



비영리. 귀하는 이 저작물을 영리 목적으로 이용할 수 없습니다.



변경금지. 귀하는 이 저작물을 개작, 변형 또는 가공할 수 없습니다.

- 귀하는, 이 저작물의 재이용이나 배포의 경우, 이 저작물에 적용된 이용허락조건을 명확하게 나타내어야 합니다.
- 저작권자로부터 별도의 허가를 받으면 이러한 조건들은 적용되지 않습니다.

저작권법에 따른 이용자의 권리는 위의 내용에 의하여 영향을 받지 않습니다.

이것은 [이용허락규약\(Legal Code\)](#)을 이해하기 쉽게 요약한 것입니다.

[Disclaimer](#)

공학석사학위논문

벽 모델 큰 에디 모사에서의
RANS 상단 경계 조건 비교

Comparison of upper boundary conditions for RANS
used in wall-modeled large eddy simulation

2017 년 8 월

서울대학교 대학원

기계항공공학부

성 창 우

벽 모델 큰 에디 모사에서의 RANS 상단 경계 조건 비교

Comparison of upper boundary conditions for RANS
used in wall-modeled large eddy simulation

지도교수 최 해 천

이 논문을 공학석사 학위논문으로 제출함

2017년 5월

서울대학교 대학원

기계항공공학부

성 창 우

성창우의 공학석사 학위논문을 인준함

2017년 6월

위원장

박형민



부위원장

최해천



위원

황원태



Comparison of upper boundary conditions for RANS used in wall-modeled large eddy simulation

Changwoo Sung

Department of Mechanical & Aerospace Engineering
Seoul National University

Abstract

The hybrid RANS/LES using zonal approach with wall shear stress model is one of the wall-modeled large eddy simulation (WMLES) techniques developed to reduce computation cost in high Reynolds number flow simulations. In this approach, how to exchange flow field information between solutions from a wall model and LES through the boundary conditions is one of the important issues. In general, the wall boundary condition of LES is given as the instantaneous wall shear stress obtained in the wall model RANS, whereas the upper boundary condition for RANS is provided as the instantaneous velocity component acquired from the solution of LES. However, it does not guarantee an accurate estimation of wall shear stress due to a resolved portion of turbulent shear stresses in RANS. In this study, a new WMLES is suggested which is directly imposing the instantaneous total shear stress obtained in LES as the upper boundary condition for RANS, rather than velocity component and assessed in turbulent channel and boundary layer flows. It is shown that the present WMLES based on the total shear stress boundary condition predicted

the logarithmic velocity profile and the low-order turbulence statistics at high Reynolds numbers even with very coarse grid resolution.

Keywords: Large eddy simulations, Wall modeling, Wall shear stress, Turbulent flows, Numerical modeling

Student number: 2011-22889

Contents

Abstract	i
Contents	iii
List of Figures	iv
Nomenclature	vii
Chapter	
1 Introduction	1
2 WMLES framework	7
2.1 Governing equations	7
2.2 Eddy viscosity model	8
2.3 Boundary conditions	9
2.4 Numerical method	10
3 Numerical Results	12
3.1 Turbulent channel flows	12
3.2 Turbulent boundary layer flows	14
3.3 Comparison with a dynamic wall model	15
4 Summary and Conclusions	26
References	28

List of Figures

Figure

1.1	A schematic diagram of the eddy viscosities modeled with each dynamic approach for the wall model RANS and the SGS eddy viscosity obtained in LES, against the wall distance (Cabot & Moin, 2000; Wang & Moin, 2002; Kawai & Larsson, 2013; Park & Moin, 2014).	6
2.1	A schematic of matching location y_m and boundary conditions of present wall modeled LES.	11
3.1	Time-averaged streamwise velocity profiles in wall units at $Re_\tau = 2003$ with different boundary conditions at the upper boundary of RANS in whole near-wall area and outer-layer region: Solid line, total shear stress boundary condition (present); dashed-dotted line, velocity component boundary condition; dashed line, $u^+ = y^+$ and $u^+ = 2.44 \ln y^+ + 5.2$; ■, DNS (Hoyas & Jiménez, 2006).	17
3.2	Time-averaged streamwise velocity profiles in wall units at $Re_\tau = 2003$ with different boundary conditions at the upper boundary of RANS near matching location: Solid line, total shear stress boundary condition (present); dashed-dotted line, velocity component boundary condition; dashed line, $u^+ = y^+$ and $u^+ = 2.44 \ln y^+ + 5.2$; ■, DNS (Hoyas & Jiménez, 2006).	18

3.3	Root-mean-square velocity fluctuations and Reynolds shear stress in wall units of LES region at $Re_\tau = 2003$: Solid line, present WMLES; ■, DNS (Hoyas & Jiménez, 2006).	19
3.4	Time-averaged streamwise velocity profiles in wall units at $Re_\tau = 2 \times 10^4$ with total shear stress boundary condition at upper boundary of RANS: Solid line, present WMLES; dashed line, $u^+ = 2.44 \ln y^+ + 5.2$	20
3.5	Time-averaged streamwise velocity profiles in wall units at $Re_\tau = 2 \times 10^5$ with total shear stress boundary condition at upper boundary of RANS: Solid line, present WMLES; dashed line, $u^+ = 2.44 \ln y^+ + 5.2$	21
3.6	Time-averaged streamwise velocity profiles in wall units with different boundary conditions at the upper boundary of RANS at $Re_\theta = 5200$: Solid line, total shear stress boundary condition (present); dashed-dotted line, velocity component boundary condition; dashed line, $u^+ = 2.44 \ln y^+ + 5.0$; ■, Experiments (De Graaff & Eaton, 2000).	22
3.7	Time-averaged streamwise velocity profiles in wall units with different boundary conditions at the upper boundary of RANS at $Re_\theta = 31000$: Solid line, total shear stress boundary condition (present); dashed-dotted line, velocity component boundary condition; dashed line, $u^+ = 2.44 \ln y^+ + 5.0$; ■, Experiments (De Graaff & Eaton, 2000).	23
3.8	Root-mean-square velocity fluctuations and Reynolds shear stress in wall units of LES region at $Re_\theta = 5200$: Solid line, present WMLES; ■, Experiments (De Graaff & Eaton, 2000).	24

3.9	Time-averaged streamwise velocity profiles in wall units with different WMLES methods at $Re_\tau = 2000$: Solid line, WMLES based on total shear stress boundary condition (present); dashed line, y -variable dynamic approach (Kawai & Larsson, 2013) with $\alpha = 0.5$; dashed-dotted line, with $\alpha = 1.2$; dashed-dot-dotted line, with $\alpha = 2.0$; fine dashed line, $u^+ = 2.44 \ln y^+ + 5.2.$, where α is a free parameter which determines level of modification of the eddy viscosity in the wall model RANS.	25
-----	---	----

Nomenclature

Roman Symbols

A^+	damping function parameter
D	near-wall damping function
h	channel half height
L	characteristic length
L_x	flat-plate length in the streamwise direction
p	non-dimensional pressure
Re	Reynolds number, UL/ν
Re_{L_x}	Reynolds number based on the flat-plate length in the streamwise direction, $u_\infty L_x/\nu$
Re_θ	Reynolds number based on the momentum thickness, $u_\infty \theta/\nu$
Re_τ	Reynolds number based on the wall shear velocity, $u_\tau h/\nu$
S_{ij}	strain rate tensor
t	non-dimensional time
U	characteristic velocity
u, v, w	non-dimensional streamwise, wall-normal and spanwise velocity components, respectively
u_∞	free-stream velocity
u_τ	wall shear velocity, $\sqrt{\tau_w/\rho}$
x, y, z	Cartesian coordinate (streamwise, wall-normal and spanwise direction, respectively)
y_{crit}	critical height in y -variable dynamic model
y_m	matching location between the wall model RANS and LES

Greek Symbols

α	free parameter in y -variable dynamics model
δ_{ij}	Kronecker delta
θ	momentum thickness
θ_0	momentum thickness at the computational inlet
κ	von Kármán constant
ν	kinematic viscosity
ν_t	eddy viscosity
ρ	density
τ_{ij}	SGS stress tensor or Reynolds stress tensor, $\overline{u_i u_j} - \bar{u}_i \bar{u}_j$
τ_w	wall shear stress

Superscripts

$()^+$	variable expressed in wall unit
$()^{\text{LES}}$	variable in LES region
$()^{\text{RANS}}$	variable in RANS region
$(\bar{ })$	spatial-filtered quantity or time-averaged quantity

Subscripts

$()_{\text{LES}}$	variable in LES region
$()_{\text{RANS}}$	variable in RANS region
$()_w$	variable at the wall

Abbreviations

DES	detached eddy simulation
DNS	direct numerical simulation
LES	large eddy simulation
RANS	Reynolds-averaged Navier-Stokes equation
rms	root-mean-square
SGS	subgrid-scale
WMLES	wall-modeled large eddy simulation

Chapter 1

Introduction

Using direct numerical simulation (DNS) or large eddy simulation (LES) to compute turbulent flows at high Reynolds numbers is prohibitively expensive due to their severe grid resolution requirements near the wall (Chapman, 1979; Choi & Moin, 2012). In terms of efficiency, applying these methods to problems of engineering interest is limited. Therefore, various techniques of wall-modeled LES (WMLES) have been suggested to reduce the number of grids near the wall by modeling the near-wall dynamics (Schumann, 1975; Cabot & Moin, 2000; Piomelli & Balaras, 2002).

According to Choi & Moin (2012), the grid requirement of LES is estimated to be proportional to $Re_{L_x}^{13/7}$, where Re_{L_x} is Reynolds number based on the flat-plate length in the streamwise direction, L_x . This is close to the grid requirement of DNS estimated in Choi & Moin (2012) that is proportional to $Re_{L_x}^{37/14}$. When directly resolving outer layer only and modeling the inner layer (rather than resolving), Choi & Moin (2012) estimated the grid point requirement is reduced to be proportional to $Re_{L_x}^1$. This suggests that WMLES is an efficient tool for prediction of high Reynolds number flow.

These WMLES approaches are classified into two categories: hybrid RANS/LES and LES with wall shear stress model, where RANS denotes Reynolds-averaged Navier-Stokes equation. The hybrid RANS/LES method fall into two categories again: the zonal approach and non-zonal approach (Piomelli & Balaras, 2002).

The first type of WMLES is the hybrid RANS/LES. This approach blends RANS using a turbulent eddy viscosity $\nu_{t,\text{RANS}}$ near the wall with LES using a subgrid-scale (SGS) eddy viscosity $\nu_{t,\text{LES}}$ away from the wall. The difference between the zonal approach and the non-zonal approach is to use a single mesh and separated grids, respectively. An example of non-zonal approach of hybrid RANS/LES is detached eddy simulation (DES) (Spalart *et al.*, 1997; Spalart, 2009). In this approach, a single turbulence model is used in a single computational grid system, and this model acts as both the RANS and LES closure models for near-wall and outer regions, respectively, corresponding to the distance from the wall. The role of this turbulence model is determined by a wall distance function. This simplicity of using a single turbulence model within a single grid makes it easy to apply DES to flows around various complex geometries. However, many recent improvements of DES include empirical parameters that makes the approach complicated (Spalart, 2009).

The second type of WMLES is the LES with wall shear stress model (Schumann, 1975; Lee *et al.*, 2013). In this approach, only the outer layer information is used for modeling the near-wall dynamics. The wall shear stress (or slip velocity), instead of no-slip, is provided as the wall boundary condition, which is obtained from outer layer information not resolving the viscous wall region. This modeling is based on that the relationship between the wall shear stress and the off-wall streamwise velocity represented by the logarithmic law of the wall. Since the assumption of the log-law in this approach may not be valid in complex flow, it is not justified to apply this approach to flows around complex geometries (Lee *et al.*, 2013; Park & Moin, 2014).

In this study, the hybrid RANS/LES using zonal approach with wall shear stress model is concerned. In this approach, an LES only resolves outer layer with very coarse grid resolution near the wall with wall shear stress boundary

condition at the wall. A wall shear stress model based on RANS is solved in only near-wall region with no-slip boundary condition at the wall, taking the instantaneous solution of LES as the upper boundary condition at a certain height above the wall. Then the instantaneous wall shear stress estimated in the wall model RANS is given back to the LES as a boundary condition at the wall. Since this method solves RANS in viscous wall region, more accurate wall shear stress can be obtained. In general, instantaneous velocity components are imposed as the upper boundary condition of the wall model RANS. However, it does not guarantee an accurate estimation of wall shear stress due to the resolved portion of turbulent stresses in the wall model (Kawai & Larsson, 2013; Park & Moin, 2014).

In order to clear up such a problem, several strategies have been suggested to improve the wall model. Most efforts are concerned with reducing resolved Reynolds shear stress in the wall model RANS by modifying the model parameter κ that determines the eddy viscosity $\nu_{t,\text{RANS}}$ of RANS with dynamic procedures. Figure 1.1 is a schematic representation of the eddy viscosities modeled with each dynamic approach for the wall model RANS and the SGS eddy viscosity obtained in LES, against the wall distance. Wang & Moin (2002) showed that the nonlinear terms in the wall model RANS increases the wall shear stress when the standard model coefficient κ is used. Cabot & Moin (2000) and Wang & Moin (2002) was obliged to reduce the eddy viscosity $\nu_{t,\text{RANS}}$ in the wall model by dynamically matching the total shear stress at the matching location y_m between LES and the wall model RANS. This strategy has been successful, but additional treatments based on the logarithmic law of the wall are required (Cabot & Moin, 2000; Wang & Moin, 2002). This is because the dynamic procedure produces too low eddy viscosity $\nu_{t,\text{RANS}}$ over the entire area of the wall model (Kawai & Larsson, 2013). Kawai & Larsson (2013) suggested

y -variable dynamic approach that uses the standard model coefficient up to a critical height y_{crit} from the wall, and uses the dynamic model coefficient varying according to the distance from the wall between y_{crit} and matching location y_m . The modified eddy viscosity in the wall model RANS $\nu_{t,\text{RANS}}$ is then maximized at y_{crit} and equal to the SGS eddy viscosity in LES $\nu_{t,\text{LES}}$ at the matching location y_m to match the total shear stress between RANS and LES at the plane. A proper wall shear stress is obtained in this modified wall model, however, additional free parameters are required in order to determine the critical blending height y_{crit} , and the optimal values of this free parameters for the best performance depends on the numerical schemes, the grid generation and the flow being simulated (Park & Moin, 2014). Recently, Park & Moin (2014) suggested an improved dynamic wall model in which the dynamic model coefficient is obtained by directly calculating the resolved portion and the modeled portion of the turbulent shear stresses from the wall model RANS, rather than by matching the total shear stress at the matching location y_m . This improved wall model provides a suitable wall boundary condition necessary for LES without introducing free parameters, but its application is limited because it requires temporal or spatial averaging (Park & Moin, 2014).

As shown above, previous studies have focused on reducing the resolved shear stress in the wall model RANS. However, the resolved shear stress which is produced in the RANS is fundamentally because the velocity components are not the same in the governing equations of RANS and LES (the governing equations are described in section 2.1). The Reynolds-averaged velocity is used in RANS and the filtered velocity is used in LES. Therefore, matching these two velocity components directly has the feasibility of error. Considering momentum transfer, it is more important to provide the stress information than to supply the velocity information. In this study, therefore, the instantaneous total shear

stress (rather than the instantaneous velocity component) estimated by the solution of LES is directly imposed as the upper boundary condition of the wall model RANS without modifying the eddy viscosity of RANS. And the proposed WMLES based on the total shear stress boundary condition at the upper boundary for the wall model RANS is assessed in turbulent channel and boundary layer flows, and compared its results with those of previous WMLES based on velocity boundary condition.

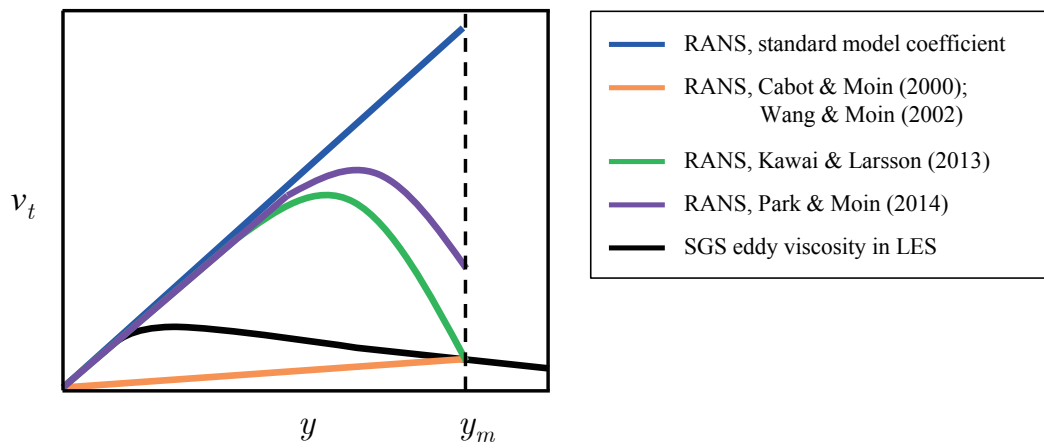


Figure 1.1. A schematic diagram of the eddy viscosities modeled with each dynamic approach for the wall model RANS and the SGS eddy viscosity obtained in LES, against the wall distance (Cabot & Moin, 2000; Wang & Moin, 2002; Kawai & Larsson, 2013; Park & Moin, 2014).

Chapter 2

WMLES framework

The present WMLES is based on hybrid RANS/LES using zonal approach with wall shear stress model. Figure 2.1 is a schematic diagram of WMLES of this study. As described above, LES resolves only the outer-layer scales away from the wall but not the viscous motions in the inner layer near the wall with very coarse grid resolution. The wall shear stress condition is applied instead of the no-slip condition as the wall boundary condition of LES. The instantaneous wall shear stress estimated in the wall model. The wall model based on RANS is solved in an auxiliary grid from the wall to a certain position away from the wall, called a matching location. This grid is embedded in LES mesh and refined in wall-normal direction only.

2.1 Governing equations

For incompressible flow, the governing equations for LES and wall model RANS are the continuity and Navier-Stokes equations,

$$\frac{\partial \bar{u}_i}{\partial x_i} = 0, \quad (2.1)$$

$$\frac{\partial \bar{u}_i}{\partial t} + \frac{\partial \bar{u}_i \bar{u}_j}{\partial x_j} = -\frac{\partial \bar{p}}{\partial x_i} + \frac{1}{Re} \frac{\partial^2 \bar{u}_i}{\partial x_j \partial x_j} - \frac{\partial \tau_{ij}}{\partial x_j}, \quad (2.2)$$

where t is the non-dimensional time, $(x_1, x_2, x_3) = (x, y, z)$ are the non-dimensional streamwise, wall-normal, and spanwise directions, respectively, $(u_1, u_2, u_3) = (u, v, w)$ are the corresponding non-dimensional velocity components, p is the non-dimensional pressure, $Re = UL/\nu$, U and L are the characteristic velocity and length, respectively, and ν is the kinematic viscosity. Here, $(\bar{\cdot})$ denotes the filtering operation for LES and Reynolds averaging operation for the wall model RANS, thus, $\tau_{ij} \equiv \overline{u_i u_j} - \bar{u}_i \bar{u}_j$ is the SGS stress tensor for LES and the Reynolds stress tensor for the wall model RANS. Note that the governing equations of RANS are for time-averaged velocity and the governing equations for LES are for spatially filtered velocity, so the velocity components of the two governing equations are different.

2.2 Eddy viscosity model

The eddy viscosity model for the stress tensor τ_{ij} is

$$\tau_{ij} - \frac{1}{3}\tau_{kk}\delta_{ij} = -2\nu_t \bar{S}_{ij}, \quad (2.3)$$

where ν_t is turbulent eddy viscosity, and \bar{S}_{ij} is the filtered strain rate tensor in LES and the Reynolds averaged strain rate tensor in the wall model RANS as

$$\bar{S}_{ij} = \frac{1}{2} \left(\frac{\partial \bar{u}_i}{\partial x_j} + \frac{\partial \bar{u}_j}{\partial x_i} \right). \quad (2.4)$$

In the LES, the SGS stress tensor τ_{ij} is determined using a dynamic global eddy viscosity model (Park *et al.*, 2006; Lee *et al.*, 2010). The eddy viscosity of LES at the first grid cell above the wall is obtained using the extension method (Cabot & Moin, 2000).

In the wall model RANS, on the other hand, the Reynolds stress tensor τ_{ij}

is modeled with a simple mixing-length eddy viscosity model with near-wall damping (Cabot & Moin, 2000) as,

$$\nu_t = \kappa y u_\tau D, \quad D = [1 - \exp(-y^+/A^+)]^2, \quad (2.5)$$

where $\kappa = 0.41$ is the von Kármán constant, y is wall-normal distance, u_τ is wall shear velocity defined as $u_\tau = \sqrt{\tau_w/\rho}$, τ_w is wall shear stress, ρ is density, D is near-wall damping function with the damping function parameter $A^+ = 17$, and y^+ is the wall-normal distance in wall units.

Most of previous studies have been involved in modifying this model coefficient κ in the eddy viscosity model in the RANS with various dynamic procedures (Cabot & Moin, 2000; Wang & Moin, 2002; Kawai & Larsson, 2013; Park & Moin, 2014) to reduce resolved shear stress in the wall model.

2.3 Boundary conditions

In the LES, the instantaneous wall shear stress τ_w is imposed as wall boundary condition. This wall shear stress is obtained in the embedded wall model RANS and is given in the horizontal directions as

$$\tau_w^{\text{LES}} = \nu \frac{\partial \bar{u}_i}{\partial y} \Big|_w^{\text{RANS}}, \quad (i = 1, 3). \quad (2.6)$$

In the wall-normal direction, $v_w^{\text{LES}} = 0$ is imposed as wall boundary condition for LES.

The wall model RANS is solved from the wall to the matching location y_m . The instantaneous total shear stress estimated by the solution of LES is directly provided as boundary condition of this matching location. Specifically, the boundary conditions are imposed as the instantaneous total shear stresses

in the streamwise and spanwise directions as

$$\left[(\nu + \nu_t) \frac{\partial \bar{u}_i}{\partial y} - \bar{u}_i \bar{v} \right]_{y_m}^{\text{RANS}} = \left[(\nu + \nu_t) \frac{\partial \bar{u}_i}{\partial y} - \bar{u}_i \bar{v} \right]_{y_m}^{\text{LES}} \quad (2.7)$$

for $i = 1, 3$, and as wall-normal velocity component $\bar{v}_{y_m}^{\text{RANS}} = \bar{v}_{y_m}^{\text{LES}}$ directly in wall-normal direction.

2.4 Numerical method

The governing equations 2.1 and 2.2 are solved using a semi-implicit fractional step method and finite volume method based on a staggered grid system: the Crank-Nicolson method and a third-order Runge-Kutta method are applied to the diffusion and convection terms, respectively (Spalart *et al.*, 1991). The second-order central difference scheme is used for the spatial discretization.

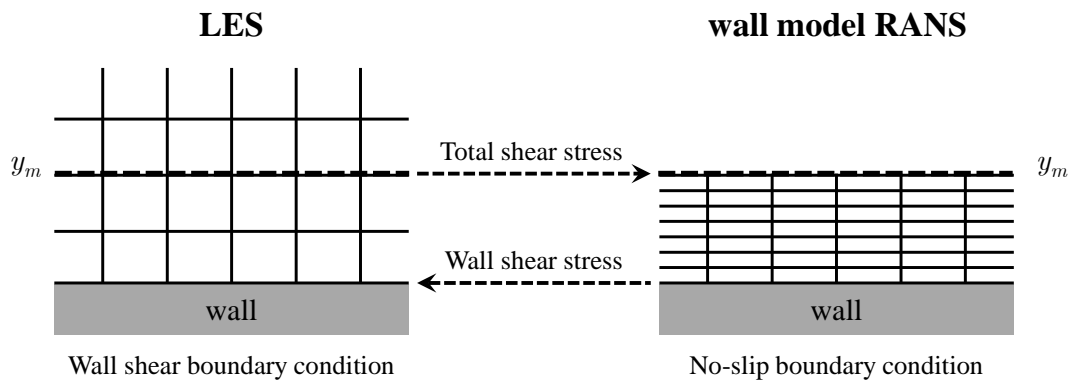


Figure 2.1. A schematic of matching location y_m and boundary conditions of present wall modeled LES.

Chapter 3

Numerical Results

3.1 Turbulent channel flows

In this section, I perform WMLES of turbulent channel flow at high Reynolds numbers imposing the total shear stress as the upper boundary condition of the wall model RANS. The Reynolds numbers considered are $Re_\tau = 2003, 4000, 2 \times 10^4$ and 2×10^5 , where $Re_\tau = u_\tau h / \nu$, and h is channel half height. The computational domain size of LES is $2\pi h(x) \times 2h(y) \times 2\pi h/3(z)$. The number of grid points used for LES is $64(x) \times 33(y) \times 32(z)$ and uniform grids are used in all directions. This domain size and grid spacings are quoted from Lee *et al.* (2013), which are comparable to those used in other studies (Lee *et al.*, 2013). For the wall model RANS, the matching plane y_m is located at fifth off-wall grid of LES as well as previous findings (Kawai & Larsson, 2012). The domain size and the number of grid points of the wall model RANS are the same as those of LES in the wall-parallel directions, and a stretched grid with 33 points in the wall-normal direction is used while keeping the size of the first off-wall grid at $\Delta y_{\min}^+ \approx 1$. In both LES and RANS, periodic boundary conditions are imposed in the streamwise and spanwise directions.

Figure 3.1 and 3.2 show the mean streamwise velocity profiles of LES and wall model RANS at $Re_\tau = 2003$ from the present WMLES based on the total shear stress boundary condition, together with those from WMLES based on

the velocity component boundary condition, the logarithmic profile, and the result from DNS (Hoyas & Jiménez, 2006). Figure 3.1 is drawn from the wall to the center plane of the channel, which includes both the near-wall region and the outer layer, and figure 3.2 is drawn to include the outer layer near matching location only. Note that both of the wall models applied here use standard model constants rather than modified model constants. The results from present WMLES show good agreements with DNS (Hoyas & Jiménez, 2006) data and the logarithmic profile in the LES region. Since the total shear stress is imposed as an upper boundary condition of the wall model RANS instead of the velocity component, the velocity discontinuity occurs at the matching location, but the wall shear stress required for the wall boundary conditions of LES can be obtained more accurately. On the other hand, the result from WMLES based on the velocity component fails to predict the logarithmic profile in the LES region, despite the continuous velocity profile is acquired due to the upper boundary condition for the wall model RANS. This indicates that the total shear stress contains appropriate momentum information necessary for the wall model RANS using a standard model constant.

In figure 3.3, the root-mean-square (rms) velocity fluctuations and Reynolds shear stress at $Re_\tau = 2003$ are shown, together with those from DNS (Hoyas & Jiménez, 2006). The turbulence statistics away from the wall show good agreements with DNS (Hoyas & Jiménez, 2006) data.

The WMLES at the higher Reynolds numbers are conducted and the mean velocity profiles are shown in figure 3.4 and 3.5. In these figure, the present WMLES also show good agreements with the logarithmic profile even at high Reynolds numbers.

3.2 Turbulent boundary layer flows

In this section, I conduct WMLES of turbulent boundary layer flow imposing the total shear stress as an upper boundary condition of the wall model RANS. The Reynolds numbers considered are $Re_\theta = 5200$ and 31000 , where $Re_\theta = u_\infty \theta / \nu$, u_∞ is the free-stream velocity, and θ is the momentum thickness. The computational domain size of LES is $600\theta_0(x) \times 40\theta_0(y) \times 50\theta_0(z)$, where θ_0 is the momentum thickness at the computational inlet. The number of grid points used in LES is $769(x) \times 65(y) \times 64(z)$ and uniform grids are used for all directions. As well as the case of turbulent channel flow, the domain size and grid spacings are also comparable to those used in other studies (Lee *et al.*, 2013). For the wall model RANS, details are almost similar to the case of turbulent channel flow. The difference is that there is only one matching plane near the lower wall (or flat plate) in the case of turbulent boundary layer flow. The matching plane y_m is located at fifth off-wall grid of LES as well as previous findings (Kawai & Larsson, 2012). The domain size and the number of grid points of the wall model RANS are the same as those of LES in the wall-parallel directions, and a stretched grid with 33 points in the wall-normal direction is used while keeping the size of the first off-wall grid at $\Delta y_{\min}^+ \approx 1$. In both LES and RANS, the recycling method (Lund *et al.*, 1998) is used to provide the inflow turbulence. The recycling location is placed $480\theta_0$ downstream of the computational inlet. A Periodic boundary condition is imposed in the spanwise direction, and a convective boundary condition is used at the computational exit as $\partial u_i / \partial t + c \partial u_i / \partial x = 0$, where c is the plane-averaged velocity at the exit. At the free-stream, the boundary conditions are given as $u = u_\infty$ and $\partial v / \partial y = \partial w / \partial y = 0$.

Figure 3.6 and 3.7 show the mean streamwise velocity profiles of LES and

wall model RANS at $Re_\theta = 5200$ and $Re_\theta = 31000$ from the present WMLES based on total shear stress boundary condition, together with those from WMLES based on velocity component boundary condition, the logarithmic profile, and results from previous experiments (De Graaff & Eaton, 2000). As with the turbulent channel flow, the results from the present WMLES show good agreements with experimental (De Graaff & Eaton, 2000) data and the logarithmic profile in the LES region, despite the discontinuity of velocity at the matching location.

In figure 3.8, the root-mean-square (rms) velocity fluctuations and Reynolds shear stress at $Re_\theta = 5200$ are shown, together with those from experiments (De Graaff & Eaton, 2000). The turbulence statistics away from the wall also show good agreements with experimental data (De Graaff & Eaton, 2000).

3.3 Comparison with a dynamic wall model

In this section, present WMLES is compared with a dynamic wall model. Several dynamic approaches have been suggested so far, and the y -variable dynamic eddy viscosity wall model (Kawai & Larsson, 2013) is known as one of the best performing methods. However, this method requires a free parameter α which determines level of modification of the eddy viscosity in the wall model RANS.

Figure 3.9 shows the mean streamwise velocity profiles of turbulent channel flow at $Re_\tau = 2000$ from the present WMLES based on total shear stress boundary condition, together with those from WMLES based on y -variable dynamic eddy viscosity wall model varying the free parameter α , and the log-law profile. Both of these two approaches show good agreements with the logarithmic profile, however, the performance of the dynamic wall model rely on the

free parameter α . Park & Moin (2014) executed similar analysis, and according to them, the optimal α depends on the numerical schemes, the grid generation and the flow being simulated. Nevertheless, the reduction of the modeled shear stress in the wall model successfully results in the appropriate wall shear stress necessary to simulate the outer-layer LES. In other words, by adjusting the wall model RANS, adequate momentum transfer occurs at the matching location. Also, this appropriate momentum transfer is achieved by only imposing the total shear stress as the upper boundary condition, without modifying the wall model.

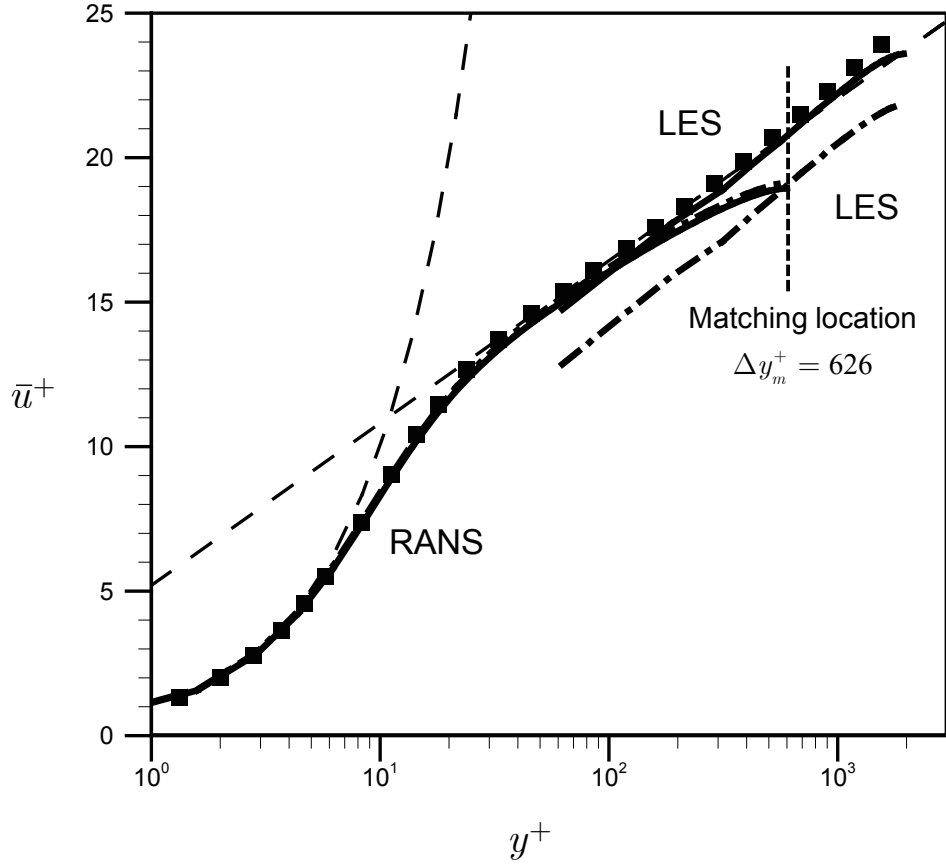


Figure 3.1. Time-averaged streamwise velocity profiles in wall units at $Re_\tau = 2003$ with different boundary conditions at the upper boundary of RANS in whole near-wall area and outer-layer region: Solid line, total shear stress boundary condition (present); dashed-dotted line, velocity component boundary condition; dashed line, $u^+ = y^+$ and $u^+ = 2.44 \ln y^+ + 5.2$; ■, DNS (Hoyas & Jiménez, 2006).

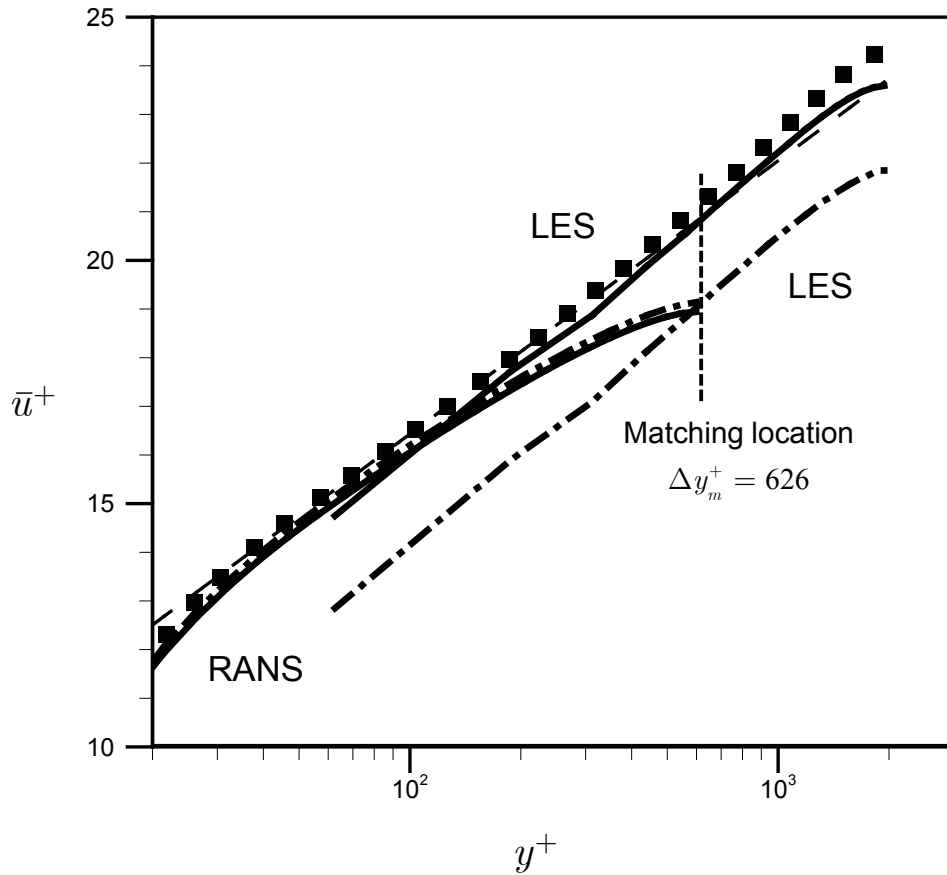


Figure 3.2. Time-averaged streamwise velocity profiles in wall units at $Re_\tau = 2003$ with different boundary conditions at the upper boundary of RANS near matching location: Solid line, total shear stress boundary condition (present); dashed-dotted line, velocity component boundary condition; dashed line, $u^+ = y^+$ and $u^+ = 2.44 \ln y^+ + 5.2$; ■, DNS (Hoyas & Jiménez, 2006).

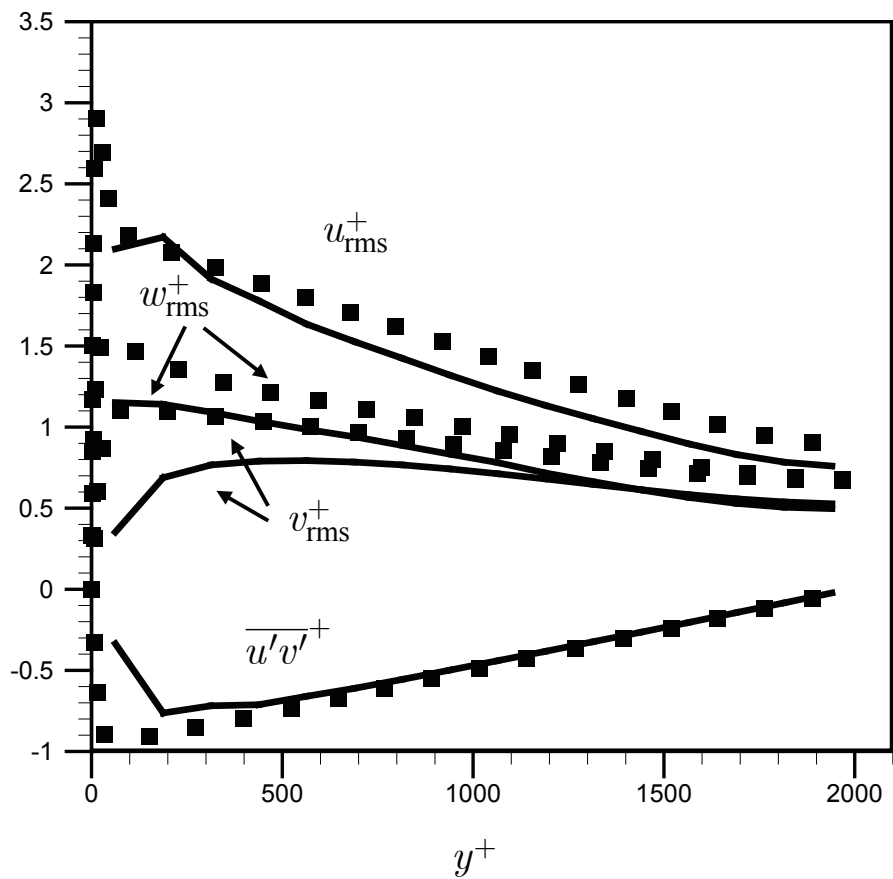


Figure 3.3. Root-mean-square velocity fluctuations and Reynolds shear stress in wall units of LES region at $Re_\tau = 2003$: Solid line, present WMLES; ■, DNS (Hoyas & Jiménez, 2006).

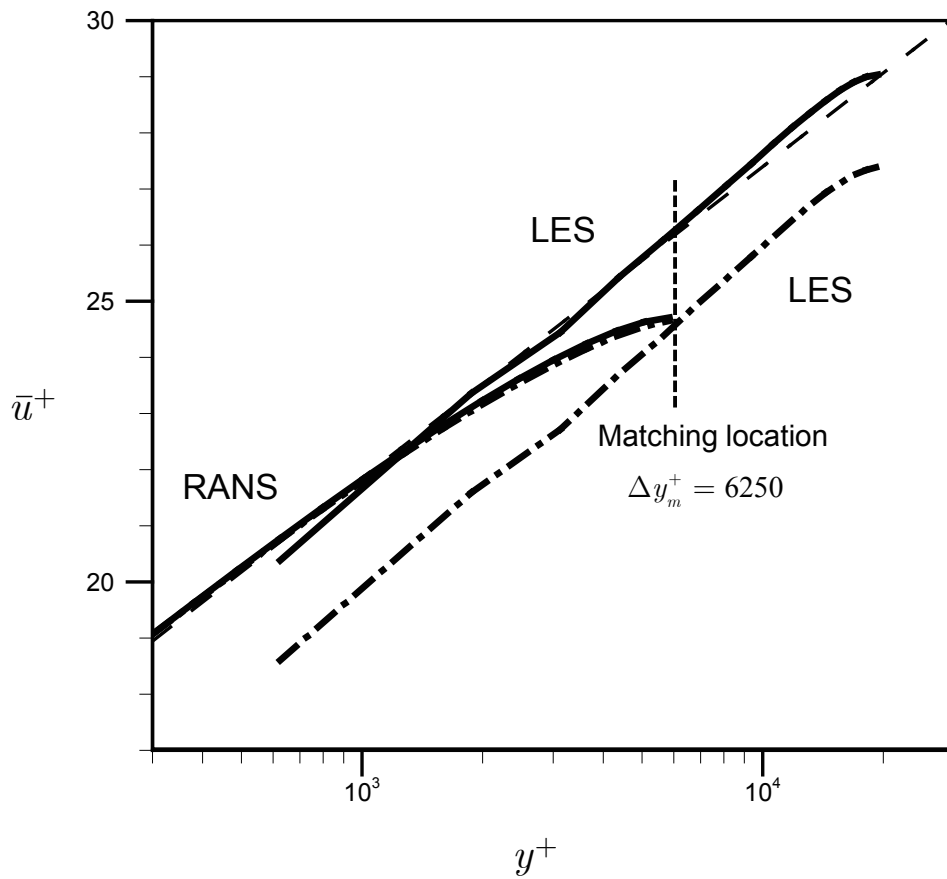


Figure 3.4. Time-averaged streamwise velocity profiles in wall units at $Re_\tau = 2 \times 10^4$ with total shear stress boundary condition at upper boundary of RANS: Solid line, present WMLES; dashed line, $u^+ = 2.44 \ln y^+ + 5.2$.

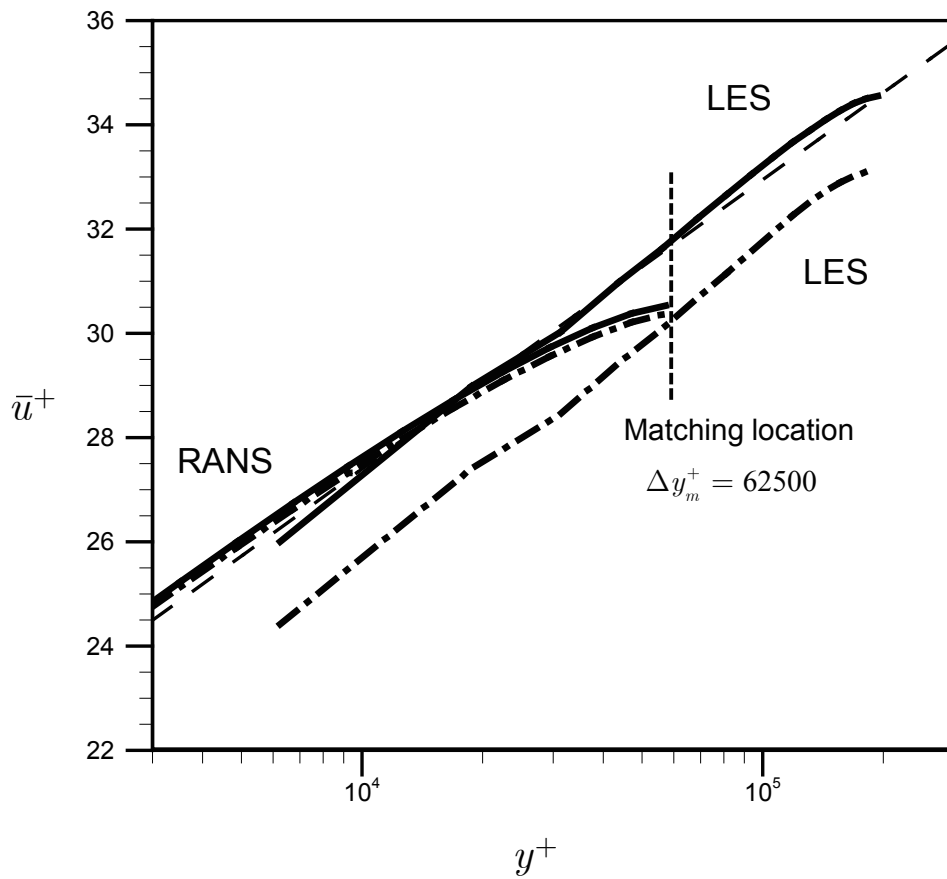


Figure 3.5. Time-averaged streamwise velocity profiles in wall units at $Re_\tau = 2 \times 10^5$ with total shear stress boundary condition at upper boundary of RANS: Solid line, present WMLES; dashed line, $u^+ = 2.44 \ln y^+ + 5.2$.

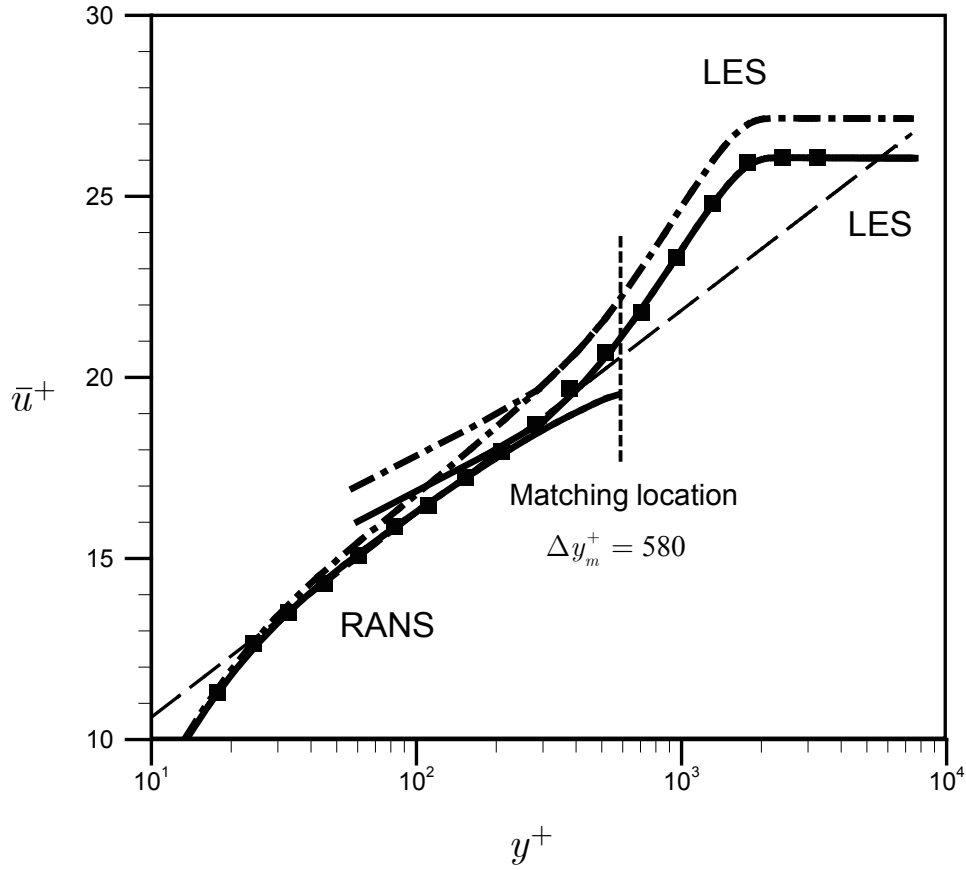


Figure 3.6. Time-averaged streamwise velocity profiles in wall units with different boundary conditions at the upper boundary of RANS at $Re_\theta = 5200$: Solid line, total shear stress boundary condition (present); dashed-dotted line, velocity component boundary condition; dashed line, $u^+ = 2.44 \ln y^+ + 5.0$; ■, Experiments (De Graaff & Eaton, 2000).

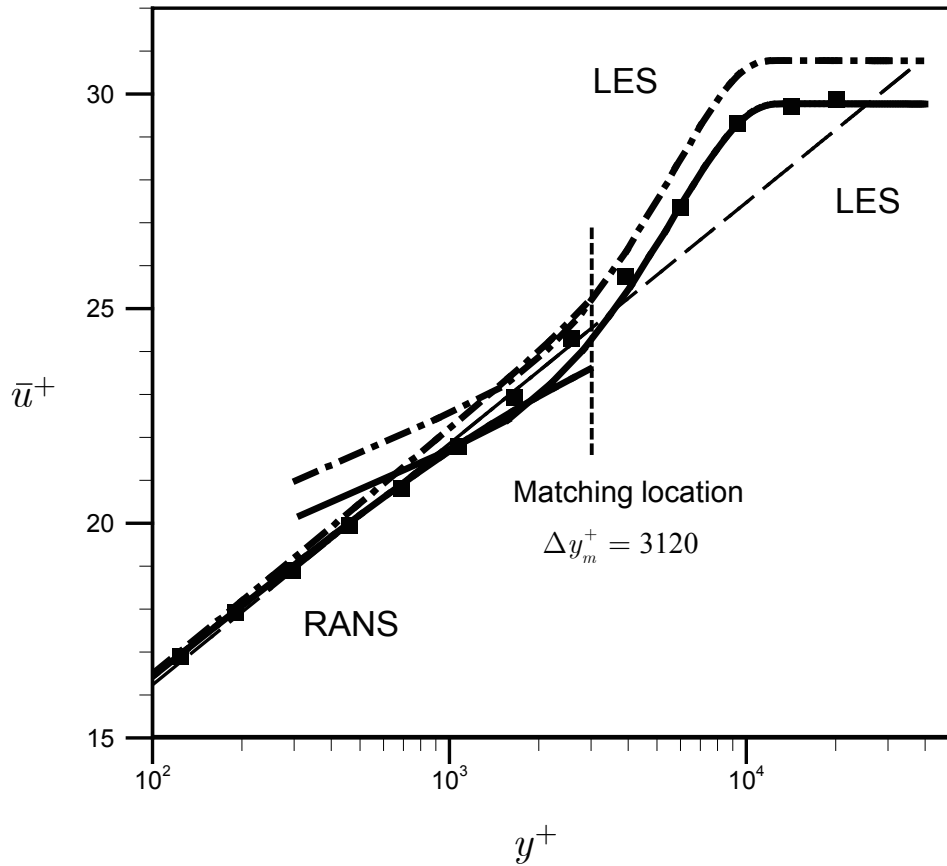


Figure 3.7. Time-averaged streamwise velocity profiles in wall units with different boundary conditions at the upper boundary of RANS at $Re_\theta = 31000$: Solid line, total shear stress boundary condition (present); dashed-dotted line, velocity component boundary condition; dashed line, $u^+ = 2.44 \ln y^+ + 5.0$; ■, Experiments (De Graaff & Eaton, 2000).

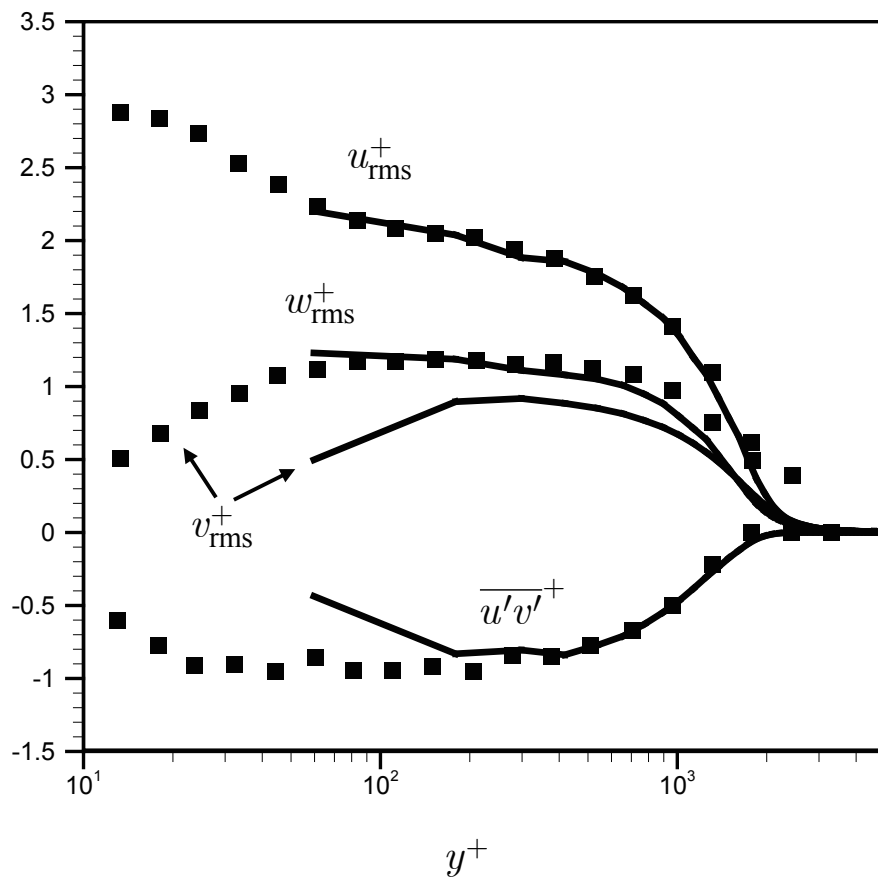


Figure 3.8. Root-mean-square velocity fluctuations and Reynolds shear stress in wall units of LES region at $Re_\theta = 5200$: Solid line, present WMLES; ■, Experiments (De Graaff & Eaton, 2000).

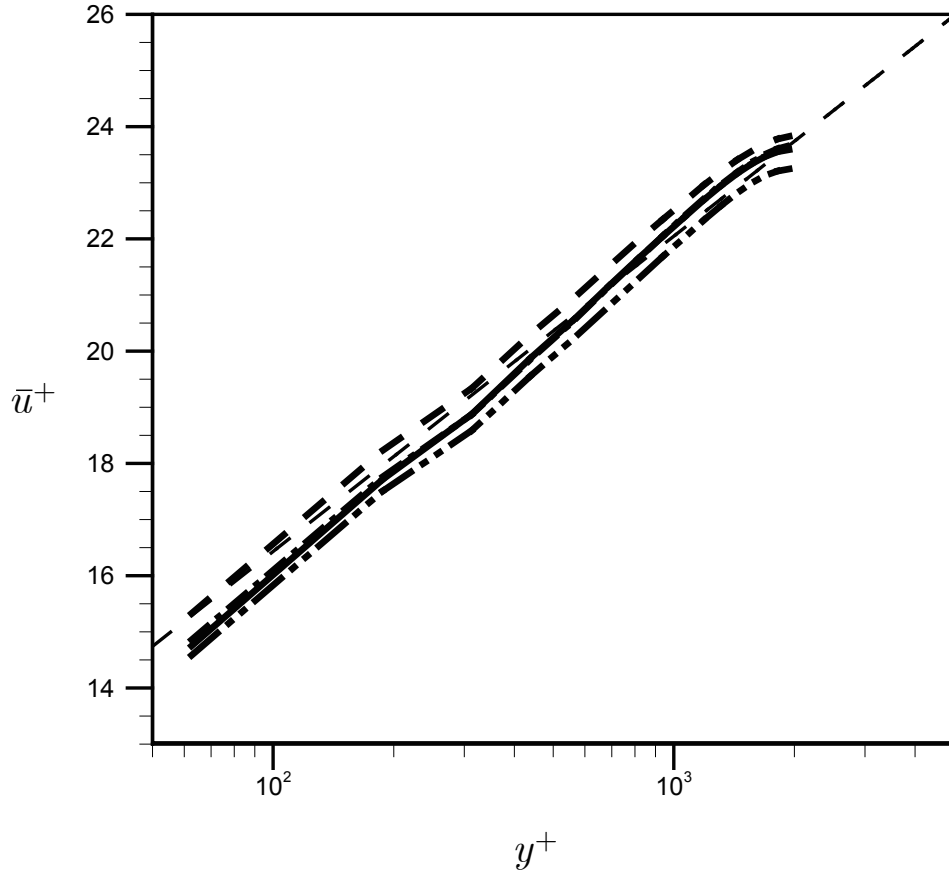


Figure 3.9. Time-averaged streamwise velocity profiles in wall units with different WMLES methods at $Re_\tau = 2000$: Solid line, WMLES based on total shear stress boundary condition (present); dashed line, y -variable dynamic approach (Kawai & Larsson, 2013) with $\alpha = 0.5$; dashed-dotted line, with $\alpha = 1.2$; dashed-dot-dotted line, with $\alpha = 2.0$; fine dashed line, $u^+ = 2.44 \ln y^+ + 5.2.$, where α is a free parameter which determines level of modification of the eddy viscosity in the wall model RANS.

Chapter 4

Summary and Conclusions

In the present study, the wall-modeled large eddy simulation was suggested which is directly imposing instantaneous total shear stress as the upper boundary condition of RANS, rather than velocity component and assessed in turbulent channel and boundary layer flows. The wall model RANS for inner-layer simulation was not modified to reduce the resolved portion of the turbulent shear stress and only the upper boundary condition for RANS were handled. It was shown that the present WMLES based on the total shear stress boundary condition predicted the logarithmic velocity profiles and the low-order turbulence statistics at high Reynolds numbers, even with very coarse grid resolution. This indicated that imposing the total shear stress as upper boundary conditions of the wall model RANS was good enough to obtain the appropriate wall shear stress, without modifying the eddy viscosity of the wall model RANS.

In the zonal hybrid RANS/LES with wall shear stress model, it is important to obtain appropriate wall shear stress necessary for LES from the wall model RANS. Compared with previous studies, it can be done by adjusting the balance of the shear stresses calculated in the wall model, and it is also possible to provide accurate stress information through the matching location as proposed in the present study. In terms of momentum transfer both approaches force the flow information of the LES obtained at the matching location to have the correct amount of momentum in the wall model RANS. Imposing the total wall

shear stress as the upper boundary condition of the wall model RANS can easily accomplish this purpose.

References

- CABOT, W. & MOIN, P. 2000 Approximate wall boundary conditions in the large-eddy simulation of high Reynolds number flow. *Flow, Turbul. Combust.* **63**, 269–291.
- CHAPMAN, D. R. 1979 Computational aerodynamics development and outlook. *AIAA J.* **17**, 1293–1313.
- CHOI, H. & MOIN, P. 2012 Grid-point requirements for large eddy simulation: Chapman’s estimates revisited. *Phys. Fluids* **24**, 011702.
- DE GRAAFF, D. B. & EATON, J. K. 2000 Reynolds-number scaling of the flat-plate turbulent boundary layer. *J. Fluid Mech.* **422**, 319–346.
- HOYAS, S. & JIMÉNEZ, J. 2006 Scaling of the velocity fluctuations in turbulent channels up to $Re = 2003$. *Phys. Fluids* **18**, 011702.
- KAWAI, S. & LARSSON, J. 2012 Wall-modeling in large eddy simulation: Length scales, grid resolution, and accuracy. *Phys. Fluids* **24**, 015105.
- KAWAI, S. & LARSSON, J. 2013 Dynamic non-equilibrium wall-modeling for large eddy simulation at high Reynolds numbers. *Phys. Fluids* **25**, 015105.
- LEE, J., CHO, M. & CHOI, H. 2013 Large eddy simulations of turbulent channel and boundary layer flows at high reynolds number with mean wall shear stress boundary condition. *Phys. Fluids* **25**, 110808.
- LEE, J., CHOI, H. & PARK, N. 2010 Dynamic global model for large eddy simulation of transient flow. *Phys. Fluids* **22**, 075106.
- LUND, T. S., WU, X. & SQUIRES, K. D. 1998 Generation of turbulent inflow data for spatially-developing boundary layer simulations. *J. Comput. Phys.* **140**, 233–258.

- PARK, G. I. & MOIN, P. 2014 An improved dynamic non-equilibrium wall-model for large eddy simulation. *Phys. Fluids* **26**, 015108.
- PARK, N., LEE, S., LEE, J. & CHOI, H. 2006 A dynamic subgrid-scale eddy viscosity model with a global model coefficient. *Phys. Fluids* **18**, 125109.
- PIOMELLI, U. & BALARAS, E. 2002 Wall-layer models for large-eddy simulations. *Annu. Rev. Fluid Mech.* **34**, 349–374.
- SCHUMANN, U. 1975 Subgrid scale model for finite difference simulations of turbulent flows in plane channels and annuli. *J. Comput. Phys.* **18**, 376–404.
- SPALART, P. R. 2009 Detached-eddy simulation. *Annu. Rev. Fluid Mech.* **41**, 181–202.
- SPALART, P. R., JOU, W. H., STRELETS, M. & ALLMARAS, S. R. 1997 Comments on the feasibility of LES for wings and on a hybrid RANS/LES approach. In *Advances in DNS/LES* (ed. C. Liu & Z. Liu), pp. 137–148. Greyden Press.
- SPALART, P. R., MOSER, R. D. & ROGERS, M. M. 1991 Spectral methods for the Navier-Stokes equations with one infinite and two periodic directions. *J. Comput. Phys.* **96**, 297–324.
- WANG, M. & MOIN, P. 2002 Dynamic wall modeling for large-eddy simulation of complex turbulent flows. *Phys. Fluids* **14**, 2043–2051.

벽 모델 큰 에디 모사에서의 RANS 상단 경계 조건 비교

서울대학교 대학원
기계항공공학부
성창우

요 약

큰 에디 모사(LES)의 벽 경계 조건으로 점착 속도 조건 대신 벽 전단 응력을 부과하는 벽 모델 큰 에디 모사(WMLES)는 벽 근처의 격자를 절감해 높은 레이놀즈 수의 유동을 예측할 수 있는 방법이다. 이에 필요한 벽 전단 응력을 구하기 위하여 벽 근처에 추가적인 격자를 도입하고 RANS와 같은 간단한 벽 모델 계산을 수행하는 혼합형 RANS/LES 방법이 있다. 이 방법에서는 경계 조건을 통한 벽 모델 RANS와 LES의 유동장 정보의 교환이 중요한 문제 중 하나이다. 일반적으로 LES의 벽 경계 조건은 벽 모델 RANS에서 얻은 순간 벽 전단 응력으로 주어지고, RANS의 상단 조건은 LES의 해로부터 얻은 순간 속도 성분으로 제공된다. 그러나 RANS의 난류 전단 응력 중 유동으로부터 유도되는 응력 성분이 존재하기 때문에 벽 전단 응력을 정확하게 구할 수 없다. 본 연구에서는 RANS의 상단 경계 조건으로 LES에서 구한 속도 성분을 부과하는 대신, LES에서 얻어진 순간 총 전단 응력을 직접적으로 부과하는 새로운 WMLES 방식을 제안하였고, 난류 채널 유동과 난류 경계층 유동에서 제안된 방식의 성능을 시험하였다. 총 전단 응력 경계 조건을 사용한 WMLES는 매우 성긴 격자를 사용하였음에도

불구하고 높은 레이놀즈 수 유동에 대하여 로그 속도 프로파일과 저차 난류 통계량을 성공적으로 예측하였다. 이를 통하여 벽 모델에 추가적인 수정을 하지 않고 RANS 상단 경계 조건으로 응력 정보를 제공하는 것으로 혼합형 RANS/LES의 성능을 개선할 수 있음을 보였다.

주요어: 큰 에디 모사, 벽 모델, 벽 전단 응력, 난류, 수치 모델링

학번: 2011-22889